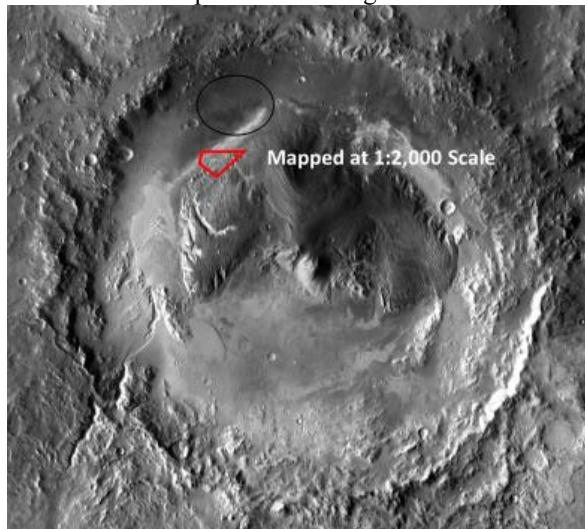


**RECOGNIZING STRATIGRAPHIC DIVERSITY THROUGH 1:10,000 SCALE GEOLOGIC MAPPING OF NORTHWEST AEOLIS MONS, MARS** A. Koepfel<sup>1</sup>, L. Edgar<sup>2</sup>, <sup>1</sup>Northern Arizona University, Department of Physics and Astronomy, Flagstaff, AZ, ak2223@nau.edu; <sup>2</sup>USGS Astrogeology Science Center, Flagstaff, AZ

**Introduction:** As the Mars Science Laboratory (MSL) Curiosity rover ascends the northwest flanks of Aeolis Mons (informally known as Mt. Sharp) in Mars' Gale crater, it has the opportunity to conduct *in situ* investigations of the diverse array of sedimentary units noted previously from orbital imagery. Measurements taken on the ground allow researchers to better constrain the validity and significance of orbital observations. Yet, in order to fully gauge how *in situ* observations may be used to ground truth orbital observations, it is imperative to generate geologic observations at multiple scales.

In this study, we bridge the gap between MSL planning-related targeted observations (1:500 scale) [1] and previously-derived geologic maps for Aeolis Mons (i.e. [1–7]) by producing a detailed 1:10,000 scale geologic map of a ~70 km<sup>2</sup> area of the mound's northwest flank. This map area is conformable with previous 1:10,000 scale mapping efforts to the north [8].

As noted in previous studies [1–12], the region contains prominent alluvial deposits and distinct channel incisions, as well as distinct finely bedded outcrops, which mark it as a prominent example for studying past conditions and depositional settings on Mars' surface.



**Figure 1.** Gale crater is ~154 km in diameter. This study's map area is outlined in red and centered at 137.3179° E, -4.8770° N. The Black ellipse represents the MSL landing ellipse (adapted from NASA/JPL).

**Methods:**

This work advances our knowledge of Aeolis Mons stratigraphy by mapping a continuous section

from the lower moat to the upper high-albedo unit at an intermediate scale. Digital mapping was carried out at 1:2,000-scale to produce a publishable map at 1:10,000-scale. This ~70 km<sup>2</sup> section, located approximately 5 km south and east of the planned MSL ascent route, offers well-exposed outcrops of the diversity of geologic units and alteration surfaces thereby providing important context for the strata that may eventually be investigated by MSL.

Mapping was conducted using 25 cm/pixel Mars Reconnaissance Orbiter High-Resolution Imaging Science Experiment (HiRISE) [13] imagery. A 1 m/pixel Digital Terrain Model produced from HiRISE stereo pairs was used as well to help identify the lateral extent of units, as well as calculate the strike and dip of bedding planes. Strike and dip measurements were acquired using the LayerTools ArcMap extension[14].

Thermal Emission Imaging System (THEMIS - ~100 m/pixel, 6.78–14.88 μm, ~1 μm/band) [15] spectral observations provided further characteristics for differentiating between units. Thermal inertia (TI) derived from THEMIS nighttime infrared observations yielded thermophysical information that was used to determine transitions in unit properties. Daytime THEMIS data (decorrelation stretch) provided a multi-band map that was used to identify changes in mineralogy. Key criteria for identifying geologic unit boundaries included major transitions in surface albedo, texture, thermal inertia, mineralogy, bedding structure and elevation.

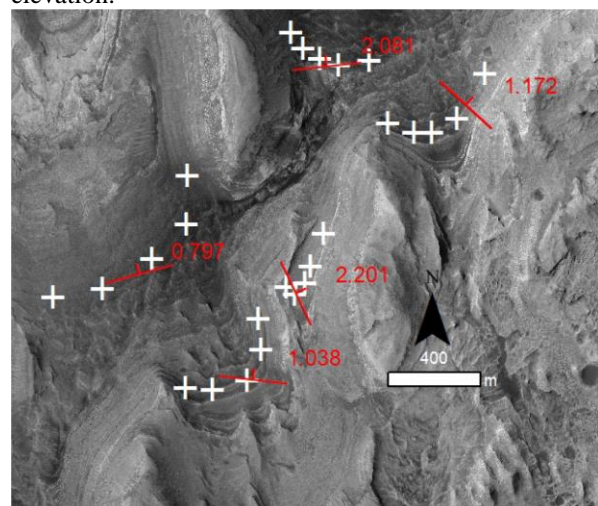


**Figure 2.** HiRISE imagery with example LayerTools strike and dip calculation. White crosses indicate locations of measured points along individual beds. Most bedding is gently dipping to the north.

**Summary:**

Based on relationships elucidated by this 1:10,000-scale map and prior works, we summarize and confirm geologic observations and interpretations for this representative vertical section of the mound.

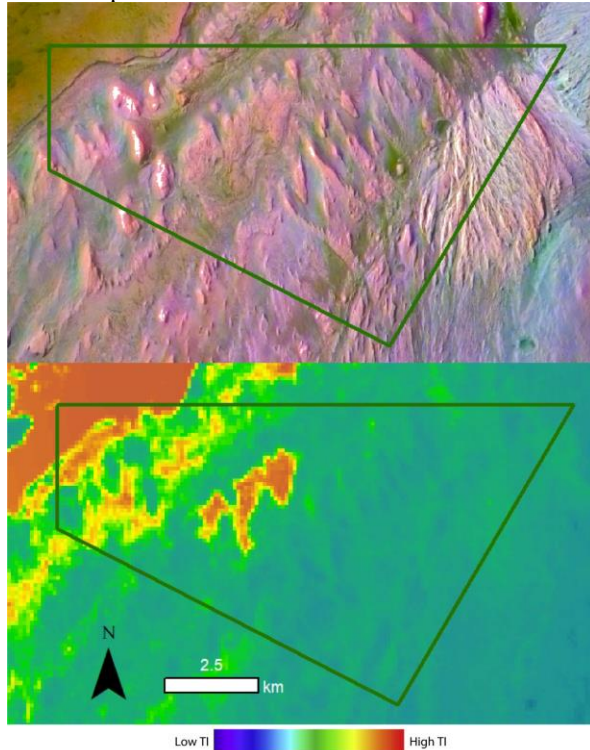


**Figure 3.** Top: THEMIS daytime IR on CTX background showing mafic minerals in yellow-green, sulfate-bearing material in pink and spectrally sloped material in blue. Bottom: qualitative TI.

This map exposes lateral variation in post-lithification process for some units, demonstrates evidence for multiple erosion-deposition episodes, and exposes some of the major variations between units adjacent units, signifying distinct environmental changes and depositional mechanism changes over time.

There is evidence for:

- Lacustrine and/or aeolian deposition was interspersed with ash fall events (marker beds) in the mound's construction.
- Episodic fluvial and/or aeolian regimes that led to vigorous erosion, evidenced by gullies, channels and yardangs.
- An up mound water source, such as melting ice, localized rain or groundwater that likely produced diagenetic alterations and induration.
- A highly cohesive (high TI) mantle that originally overlay some of the mound, but has since

eroded to the mound's base, as evidenced by dip measurements and unit contacts.

- Bright aeolian deposits higher in the mound that unconformably overlie previously eroded and cratered sediment.

Through detailed geologic mapping this work identifies a number of new units in the lower mound that may indicate more variability in the depositional and erosional history than previously identified. This work provides observations that may be used to further support ongoing science at the central mound within Gale crater.

**References:**

- [1] Stack, K.M. *et al.* (2017). in *LPSC XLVIII*. [2] Anderson, R. & Bell III, J.F. (2010) *Mars Int. J. Mars Sci. Explor.* 5 (76–128). [3] Deit, L. Le *et al.* (2013) *JGR Planets* 118 (2439–2473). [4] Fraeman, A.A. *et al.* (2016) *JGR Planets* 121 (1713–1736). [5] Milliken, R.E. *et al.* (2010) *GRL* 37 (1–6). [6] Thomson, B.J. *et al.* (2011) *Icarus* 214 (413–432). [7] F. J. Calef III *et al.* (2016). in *PGM* (7040). [8] L. A. Edgar *et al.* (2017). in *LPSC XLVIII*. [9] Siebach, K.L. & Grotzinger, J.P. (2014) *JGR Planets* 119 (189–198). [10] Schwenzer, S.P. *et al.* (2012) *Planet. Space Sci.* 70 (84–95). [11] Kite, E.S. *et al.* (2013) *Icarus* 223 (181–210). [12] Kite, E.S. *et al.* (2013) *Geology* 41 (543–546). [13] McEwen, A.S. *et al.* (2007) *JGR Planets* 112 (E05S02). [14] Kneissl, T. *et al.* (2010) *LPSC XLI* (1640). [15] Ferguson, R.L. *et al.* (2006) *JGR Planets* 111 (1–22).